2 August 2015
Data Version 4.0

Aquarius Salinity Validation Analysis; Data Version 4.0

Lead Authors: Gary Lagerloef (Earth & Space Research), Aquarius Principal Investigator, and Hsun-Ying Kao (Earth & Space Research)
Contributing Authors: Thomas Meissner (Remote Sensing Systems), Jorge Vazquez (JPL/Caltech)

1. Introduction

The purpose of this report is to document the Aquarius sea surface salinity (SSS) measurement error statistics and some residual errors in the **V4.0** data release (July 2015). We also document the effect that changes in the science data processing from V2.0, V3.0 to V4.0 and present the error statistics by comparing V2.0, V3.0 and V4.0 results. It should be noted that V3.0 (released in July 2014) contained a significant latitude-dependent bias (positive bias in high latitudes and negative in low latitudes). The bias was found to be correlated with SST, and accordingly, an SST-adjustment was provided in the V3.0 data. As attention focus on the cause of the V3.0 biases, a comprehensive V3.0 validation analysis was never fully documented. By including some V3.0 calculations in this document, some supplementary, though incomplete, V3.0 documentation is now provided.

In this analysis, we used an interim test data set named V3.6, which is the same processing code that is used for V4.0. Accordingly, all the analyses and figures here refer to V4.0 when in fact the calculations were done with V3.6 test data files. Here we use 31 months of V2.0 data (from Sep 2011 to Mar 2014, when V2.0 processing stopped) and 41 months of V3.0 and V4.0 data (from Sep 2011 to Jan 2015) for comparison.

Readers of this document are assumed to be familiar with the Aquarius/SAC-D mission and sensor design, sampling pattern, salinity remote sensing principles, and pre-launch error analysis as described by [1] and [2]. It is particularly relevant to the error analyses to understand that the measurement sensitivity decreases with decreasing sea surface temperature (SST), so that the salinity data are more prone to errors in the high latitudes than in the tropics. The information is documented in [3].

The sensor calibration is done with a forward model to estimate the antenna temperature at the satellite, then differencing that estimate from the measured antenna temperature on a global average [4]. The forward model includes the surface emission, geophysical corrections, antenna pattern correction, etc. The surface emission for the forward model is derived from ancillary SST and SSS. The SST data are derived from the daily high-resolution blended SST produced by NOAA National Center for Environmental Prediction (NCEP) as described in [5]. The SSS are derived from the US Navy HYbrid Coordinate Ocean Model (HYCOM) daily averaged data –assimilative analysis ([6] and Appendix A). The operational data are distributed by the U.S. Naval Oceanographic Office (NAVO), but the digital output are distributed by Florida State University. HYCOM salinity is used as a global surface calibration target for the sensor, whereas validation of the salinity output is done with surface *in situ* buoy data, primarily Argo floats. The basic principle, therefore, is to *calibrate* with HYCOM globally, and *validate* with buoy data locally, although HYCOM salinity is also considered with buoy data in some of the global statistical error analyses.

An important achievement in the V3.0 data is a better correction for the reflected galaxy. This has greatly reduced the amplitude and the seasonal variation of the ascending and descending differences, particularly in the Southern Ocean. However, V3.0 shows noticeable positive biases in the high latitude. As a result, negative biases show up in the low latitude after the calibration to the global mean with HYCOM data. The salty biases at high latitude (in particular in the North Pacific) are correlated to SST, possibly surface roughness or air-sea temperature difference or a combination of these. In V4.0, the regional bias has been significantly reduced with an updated geophysical model function (GMF) to correct SST and wind effect on roughness. The thresholds used for flags are also revised to exclude the outliers more efficiently (see Section 4.2 in the Aquarius Level-2 Data Product, Version 4.0).

The Aquarius project produces three data sets: Level 1a (raw data), Level 2 (science data in swath coordinates and matching ancillary data), and Level 3 (gridded 1-degree weekly and monthly salinity and wind speed maps). This validation analysis will start with Level 2 data evaluation followed by Level 3 on monthly and seasonal (3-month) averages. Salinity measurements are on practical salinity scale (PSS-78), technically a dimensionless number, but in some figures labeled as practical salinity units (psu). In this version, we also add density in the variables. More details are described in Section 11.

2. Matchup maps and differences (V2.0, V3.0 & V4.0)

We start with global maps comparing the Aquarius Level 2 samples with surface *in situ* data, including Argo buoy and global tropical moored buoy array from Pacific Marine Environmental Laboratory (PMEL) (Figure 1). The Argo data are generally sampled at a shallowest depth of 3-5 meters from the surface, and the buoy array from PMEL can be as shallow as 1 meter deep. Under most conditions (e.g., moderate to high winds, the surface ocean mixed layer extends much deeper, and

the buoy provides an accurate measure of the 1-2 cm surface layer that emits the microwave signal seen by the satellite. However, under persistently rainy conditions, there are often gradients between the surface and the buoy measurement depth. The Aquarius Level 2 (swath) data are taken at the closest point to a buoy. The time window is ± 4.5 days to gather all buoy data within the 7-day orbit repeat cycle. The search radius is 75 km between the buoy location and the bore sight position of the Aquarius footprint. The Aquarius data are averaged over 11 samples (~100 km) centered on the match-up point. Argo buoys surface once every 10 days and remain at the surface for a few hours. The data are collected randomly at any time of the day.

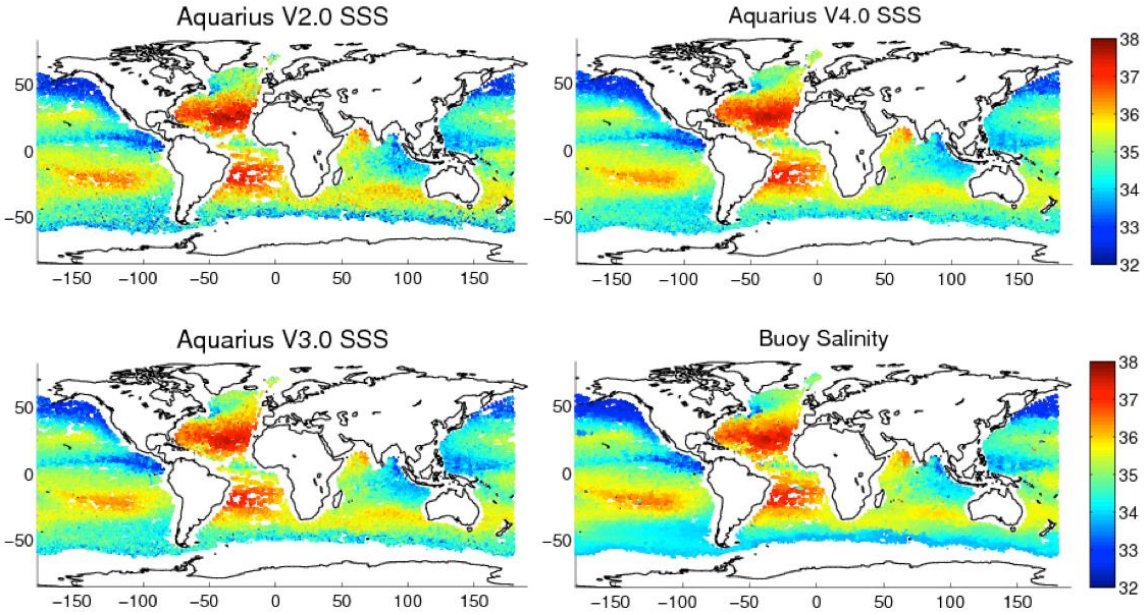

Figure 1. Aquarius and buoy co-located salinity data

Figure 1 shows the Aquarius retrieved salinity at the buoy matchup points for 31 months of V2.0 and 41 months of V3.0 and V4.0 observations. Aquarius V4.0 data and the buoy data at the same matchup points are shown. The correspondence is visibly quite clear with Aquarius Level 2 data resolving the salient large-scale ocean features. The major noise in V2.0 in the extreme southern latitudes is significantly reduced in V3.0 and V4.0. The reduced biases in the Southern Ocean are mainly due to the improved roughness correction. In V3.0 and V4.0, Aquarius HHH winds are used to replace the NCEP winds, which are used in V2.0.

Figure 2 shows the Aquarius – *in situ* differences with these same match-ups for V2.0, V3.0 and V4.0. One conspicuous improvement evident in V4.0 is in reducing the large noise that V2.0 has in the Southern Ocean. Other systematic improvements less visible here will be demonstrated by related analyses below.

The latitudinal bias is observed in V4.0, with negative bias in the low latitude and positive bias in the high latitude, but the values are smaller than 0.2 psu. See Section 7 for more discussion about the latitudinal bias.

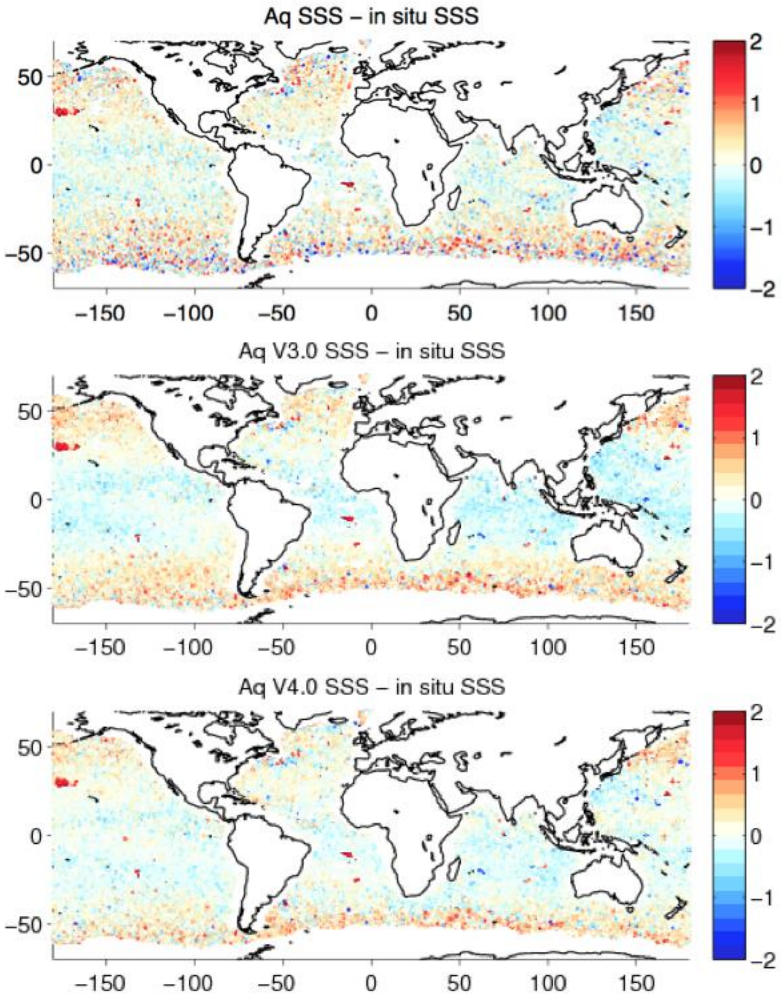

Figure 2. Global maps of SSS differences as defined by the Aquarius V2.0 (top), V3.0 (middle) and V4.0 (bottom) data minus the co-located buoy data.

3. 3-beam histograms (V2.0, V3.0 & V4.0)

Histograms of the matchup salinity differences for each of the three beams are in Figure 3. In these statistics, we use moderate flags to exclude colocations that add considerable noise and skewness to the data (SST < 5°C, windspeed > 15 m/s, and gain-weighted land and ice fractions > 0.001). There is a measureable reduction of the standard deviations in all three beams mainly due to the replacement of the wind product from NCEP to Aquarius HHH winds. The root mean square difference (RMSD), which is the root sum square (RSS) of the bias and standard deviation, is reduced from **~0.51** in V2.0 to **~0.39** in V3.0 and **~0.35** in V4.0. These are the ensemble statistics for the 31-month (Sep 2011 to Mar 2014) and 41-month (Sep 2011 to Jan 2015) record of global ice-free ocean data.

Scatter plots between the Aquarius and buoys are shown for each beam in Figure 4. The color contours represent the density of points, and fit is quite linear over the open ocean salinity dynamic range. Evident outliers at about 34 psu in V2.0 are reduced in V4.0, being less biased in the high latitudes. Generally, the salinity

observations are more concentrated to the 1:1 ratio in V4.0, representing the overall smaller biases in V4. 0.

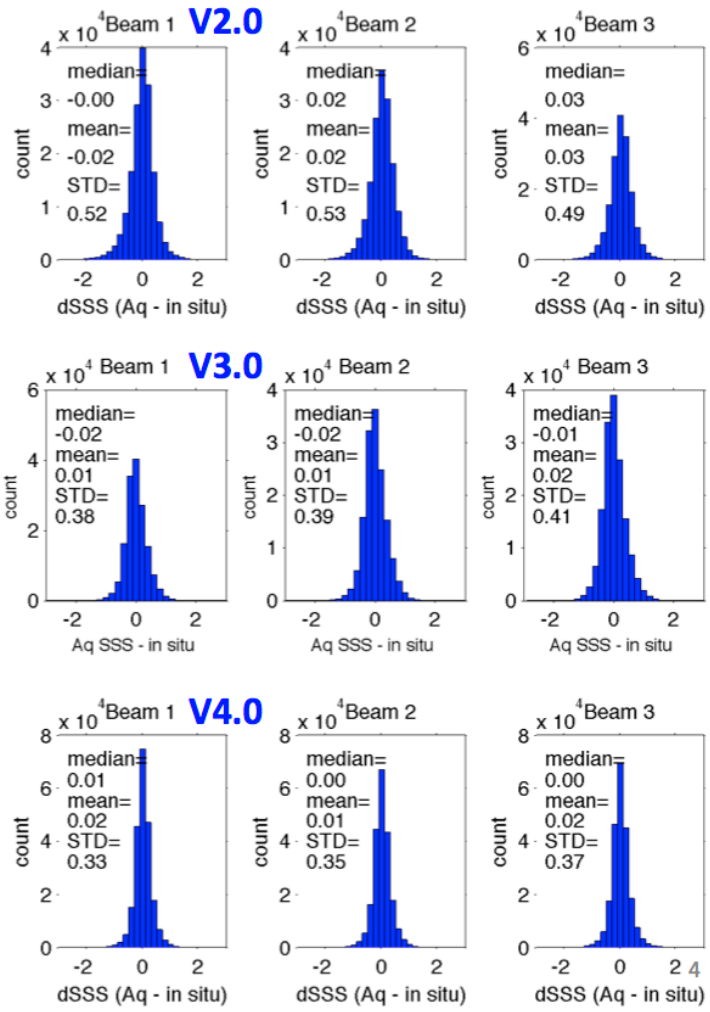

Figure 3. Histograms for Aquarius – buoy differences, V2.0 (top), V3.0(middle) and V4.0 (bottom).

The HYCOM data are used as a salinity reference for evaluation and global calibration [4]. The HYCOM surface salinity is interpolated to the time and location of every 1.44 second sample interval in Aquarius Level 2 data files. Here, in Figure 5, these reference salinity data are evaluated against the Argo measurements with the same matchup processing as Aquarius Level 2 data. The results are shown separately for the ascending (northward) and descending (southward) halves of the orbit. The first feature to emphasize in Figure 5 is that there is no systematic difference between the ascending to the descending passes for the buoy and HYCOM salinity difference. This continuity is noteworthy because of the ascending – descending differences found in V2.0 has been greatly reduced in V4.0 and results are addressed in detail in Section 7. Secondly, it is clear that there are regional long-term systematic biases between HYCOM output and the buoy data. HYCOM is biased positive relative to the in situ in the Antarctic circumpolar current, tropics and north Pacific. Over much of the mid latitudes the bias is slightly negative. These differences exist even though most of the in situ data we are using here are assimilated by HYCOM and therefore not fully independent data.

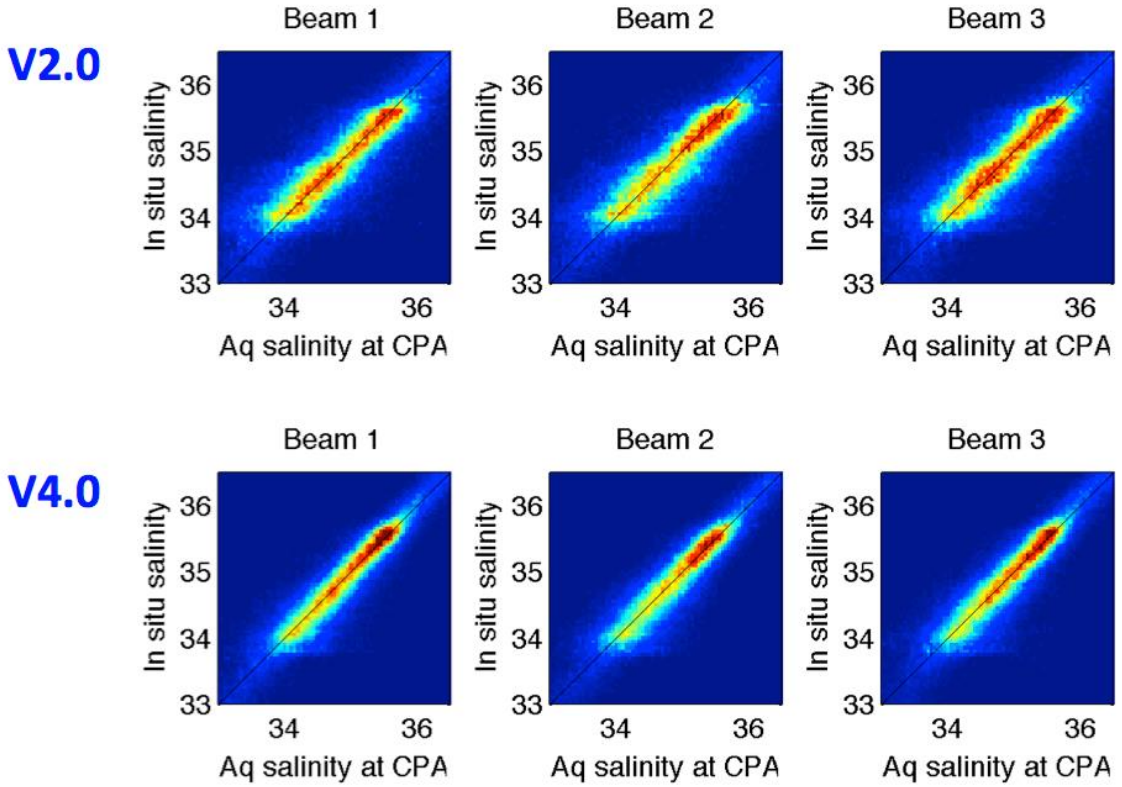

Figure 4. Scatter plots of V2.0 and V4.0 Aquarius (abscissa) and co-located buoy data (ordinate) for each beam.

The histograms and statistics in Figure 5 demonstrate that for the global average, the HYCOM-buoy differences have no bias, either for ascending or descending passes. This is a relevant point for validating our overall calibration approach because we use the HYCOM salinity as a surface reference for modeling the on-orbit antenna temperature for calibrating the sensors [4]. We compute these calibrations on a global scale with running averages that use all orbits in a 7-day repeat cycle. In contrast, the HYCOM-buoy regional differences demonstrate that regional or zonal calibrations will be problematic, and we have used only global analyses for calibration.

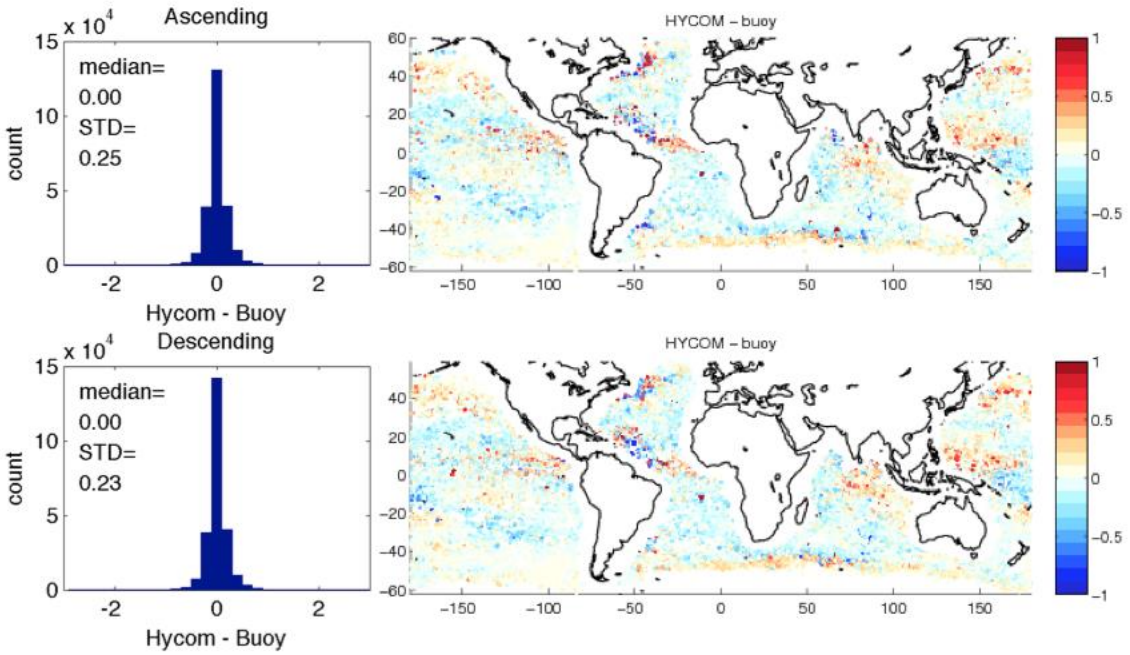

Figure 5. Co-located salinity differences between HYCOM and buoys for ascending (top) and descending (bottom) passes.

4. Triple point analysis

Figure 6 gives the V4.0 matchup statistics for Aquarius – buoy, HYCOM – buoy, and Aquarius – HYCOM (at the buoy locations), for each of the three beams. The global bias between the data is small, so the RMSD is essentially the same as the STD. These show HYCOM – buoy RMSD ~0.24 overall. The RMSD for Aquarius – buoy is slightly higher than the RMSD for Aquarius – HYCOM (~0.03). The co-located statistics allow us to estimate the root mean square error (RMSE) of each of the three measurements (*See Appendix A*). These results are given in Table 1, where the Aquarius RMSE are ~0.28 (which was ~0.46 in V2.0) and the HYCOM and buoy RMSE are ~0.15 and ~0.20, respectively. Recall that these Aquarius matchup statistics are for individual measurements, with no averaging. The idealized monthly average RMSE is possibly as low as ~0.10, assuming a minimum of 8 samples per month and uncorrelated errors, as seen in the lower panel of Table 1. Directly computed monthly statistics are not this small, as will be discussed in Section 6.

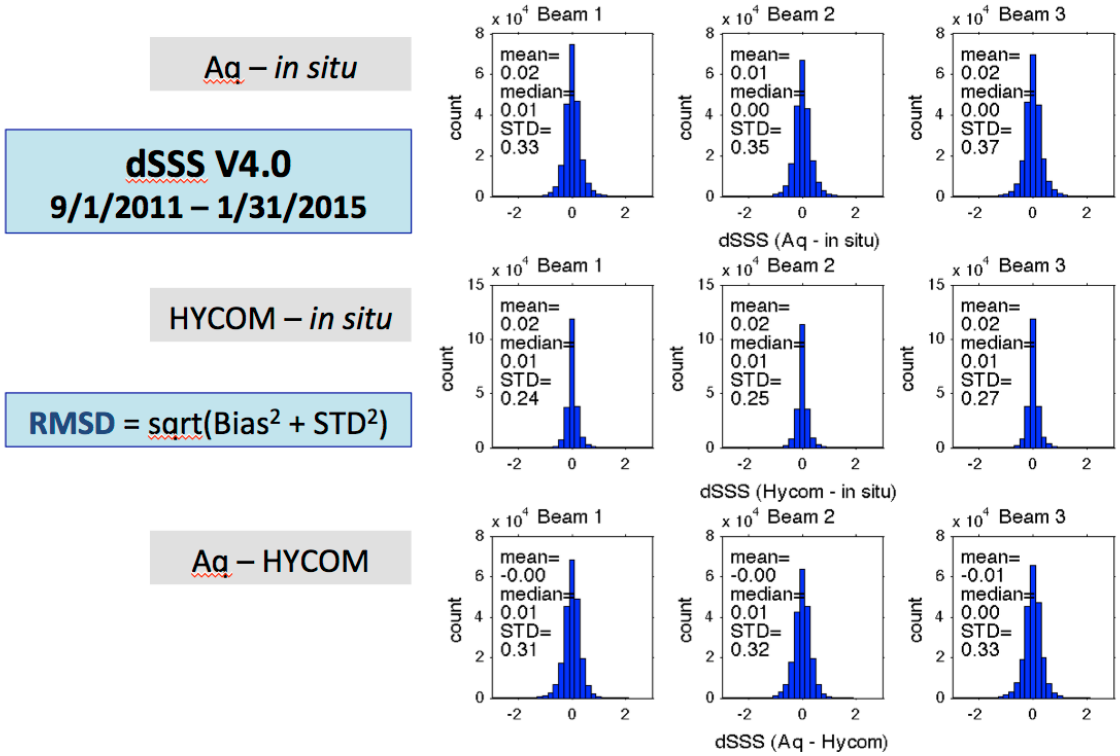

Figure 6. Co-located difference histograms for each beam and Aquarius V4.0 data. (top) Aquarius – *in situ*, (middle) HYCOM – *in situ*, (bottom) Aquarius – HYCOM.

Table 1. Estimated Root Mean Square Error (RMSE) for each data type based on the triple point analysis of co-located point measurements.

	Beam 1	Beam 2	Beam 3
Aquarius RMSE	**0.27**	**0.29**	**0.29**
HYCOM RMSE	**0.15**	**0.15**	**0.15**
***In situ* RMSE**	**0.19**	**0.20**	**0.22**
Theoretical monthly RMSE if all errors are uncorrelated.			
Monthly RMSE (8 samples worst case) psu	0.10	0.10	0.10

5. Buoy matchup time series (V2.0, V3.0 & V4.0)

A key milestone in V3.0 and V4.0 data processing relates to galaxy correction. Figure 7 shows the global average salinity bias over time. V3.0 shows similar results as V4.0 (bottom). These time series curves are global daily median values of Aquarius-buoy matchup data. Although the quasi-monthly wiggles in V1.3 are gone in V2.0,

the V2.0 time series does show smaller calibration drifts with near-annual time scale. V4.0 data extending to longer time period show that these have been effectively removed. The updated flags in V4.0 also reduced the spikes in the time series.

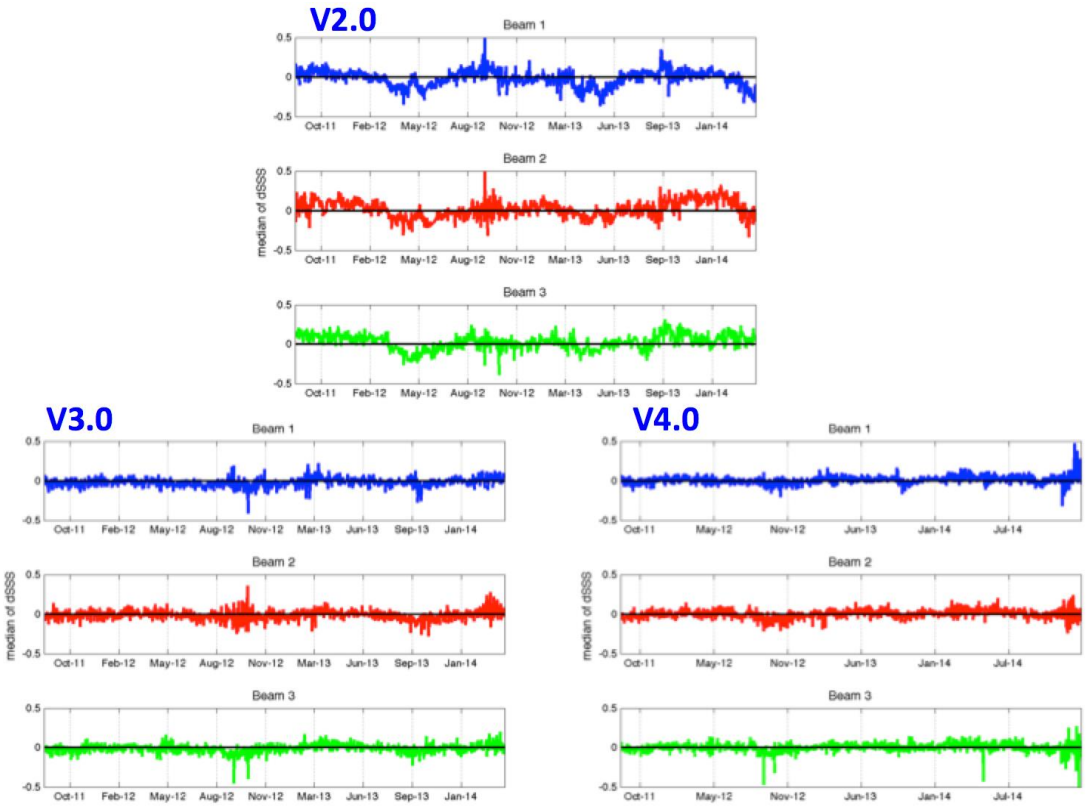

Figure 7. Daily global average Aquarius-buoy difference time series, V2.0 (upper), V3.0 (bottom left) and V4.0 (bottom right).

6. Monthly and seasonal buoy matchup maps

Next, we examine buoy difference statistics of monthly 1x1 degree Level 3 salinity data maps. The Level 3 maps are generated from Level 2 salinity data without any added adjustment for climatology, reference model output or *in situ* data. The smoothing interpolation applies a bi-linear fit within a specified search radius. Most of the results shown here are computed using a ~150km radius, and exclude data where land or ice fractions exceed 0.001 (ESR data), which are restricted to open ocean. The buoy matchups are compiled for each 1-degree grid with an average of the buoys within the 150 km radius and with buoy SST >5°C.

Results for V3.0 are shown in Table 2 and for V4.0 data are shown in Table 3 and Figure 8. The tabulated monthly standard deviations range from 0.14 to 0.29 from Sep 2011 to Aug 2014. The standard deviations in V3.0 are considerably less than V2.0 (range from 0.42 to 0.54) and even less in V4.0. The evident positive bias in the Southern Hemisphere from September 2011 to February 2012 observed in V2.0

(see Aquarius validation document for V2.0) can still be seen in V3.0 and V4.0, but the amplitude has been significantly reduced. The negative bias throughout the tropics observed in V2.0 is more confined under the ITCZ in V3.0/V4.0 with more reasonable value that is closer to the differences caused by the stratification near the surface.

The standard Aquarius Level 3 data produced by the Aquarius Data Processing System (ADPS) using the same algorithm with different flags for excluding data from the gridding. In V.4 ADPS data, the criterion for land fraction is set as 0.01 (severe) to include more data points in the global maps. As a result, the standard deviations are much higher (>0.30) compared to the gridding using 0.001 (moderate) for land fraction.

Table 2. V3.0 Aquarius monthly difference statistics (ESR).

	median	RMS		median	RMS		median	RMS
SEP/11	0.04	0.26	SEP/12	-0.03	0.29	SEP/13	0.00	0.28
OCT/11	-0.01	0.29	OCT/12	-0.02	0.33	OCT/13	0.00	0.29
NOV/11	0.03	0.31	NOV/12	-0.01	0.31	NOV/13	0.01	0.27
DEC/11	-0.01	0.27	DEC/12	-0.02	0.26	DEC/13	0.00	0.25
JAN/12	-0.01	0.25	JAN/13	-0.01	0.24	JAN/14	0.01	0.25
FEB/12	0.00	0.25	FEB/13	0.03	0.23	FEB/14	0.03	0.28
MAR/12	-0.01	0.24	MAR/13	0.05	0.23	MAR/14	0.04	0.33
APR/12	-0.01	0.28	APR/13	0.06	0.26	APR/14	0.03	0.38
MAY/12	0.02	0.28	MAY/13	0.06	0.25	MAY/14	0.04	0.31
JUN/12	0.01	0.28	JUN/13	0.04	0.26	JUN/14	0.04	0.31
JUL/12	-0.01	0.25	JUL/13	0.03	0.24	JUL/14	0.01	0.30
AUG/12	-0.02	0.25	AUG/13	0.02	0.26	AUG/14	0.02	0.32

Table 3. V4.0 Aquarius monthly difference statistics (ESR).

	median	STD		median	STD		median	STD
SEP/11	0.00	0.19	SEP/12	0.00	0.22	SEP/13	0.01	0.21
OCT/11	0.00	0.21	OCT/12	0.00	0.21	OCT/13	0.01	0.20
NOV/11	0.01	0.23	NOV/12	-0.01	0.24	NOV/13	0.01	0.21
DEC/11	0.00	0.22	DEC/12	-0.01	0.21	DEC/13	0.01	0.22
JAN/12	0.00	0.19	JAN/13	0.00	0.20	JAN/14	0.01	0.18
FEB/12	0.02	0.19	FEB/13	0.01	0.18	FEB/14	0.02	0.21
MAR/12	0.01	0.19	MAR/13	0.01	0.15	MAR/14	0.03	0.23
APR/12	-0.01	0.21	APR/13	0.00	0.14	APR/14	0.03	0.26
MAY/12	0.00	0.22	MAY/13	0.00	0.16	MAY/14	0.04	0.25
JUN/12	-0.01	0.25	JUN/13	0.00	0.15	JUN/14	0.03	0.29
JUL/12	-0.01	0.21	JUL/13	0.00	0.19	JUL/14	0.03	0.26
AUG/12	0.00	0.20	AUG/13	0.00	0.17	AUG/14	0.03	0.24

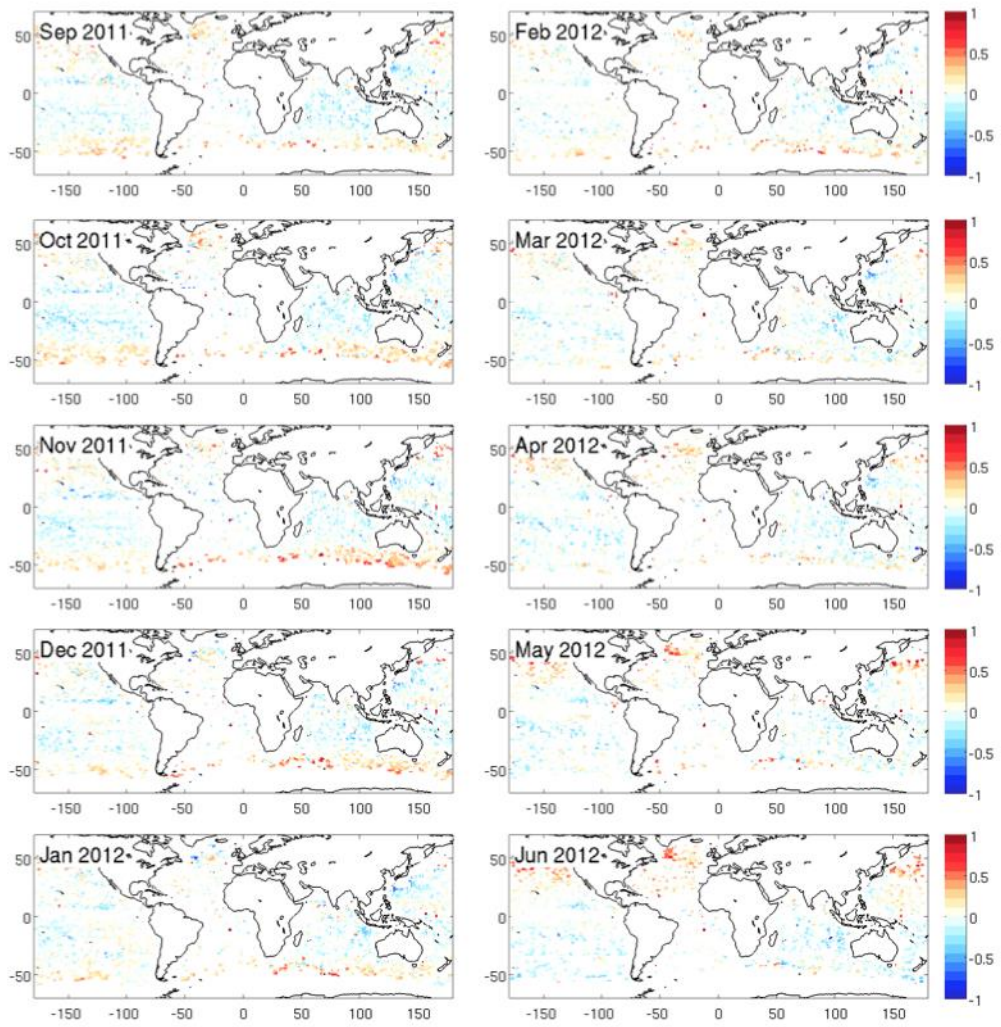

Figure 8. V4.0 Aquarius monthly difference maps.

7. Contrasting ascending and descending passes

We now examine the differences between the ascending (northward, 6pm) and descending (southward, 6am) with ADPS L3 data. These show the improvement of V4.0 data related to the galaxy correction, antenna pattern correction and improved setting of the flags. In principle, the ascending and descending maps are expected to be nearly identical (e.g. Figure 5). Here we use a 31-month block of data from September 2011 through March 2014 for V2.0. The ascending-descending map for V2.0 (Figure 9) shows several areas of concern with biases much in excess of 0.2 psu. In the Northern Hemisphere, a large blue patch in the eastern Atlantic, and red zones in the western Atlantic and Asian Pacific are believed to be related to low-level ratio frequency interference (RFI) from adjacent land areas that leaks through the antenna side lobes and is not detected by the standard RFI filter algorithm. This causes a positive brightness temperature bias and thus a negative salinity bias. The RFI asymmetry between ascending and descending is the results of the opposite viewing angle (toward or away from the land emitting sources) between the two

sides of the orbit. The antenna faces eastward on ascending passes and westward on descending passes. The Southern Hemisphere biases are likely to be related to the galaxy reflection term that is not correctly adjusted for wind.

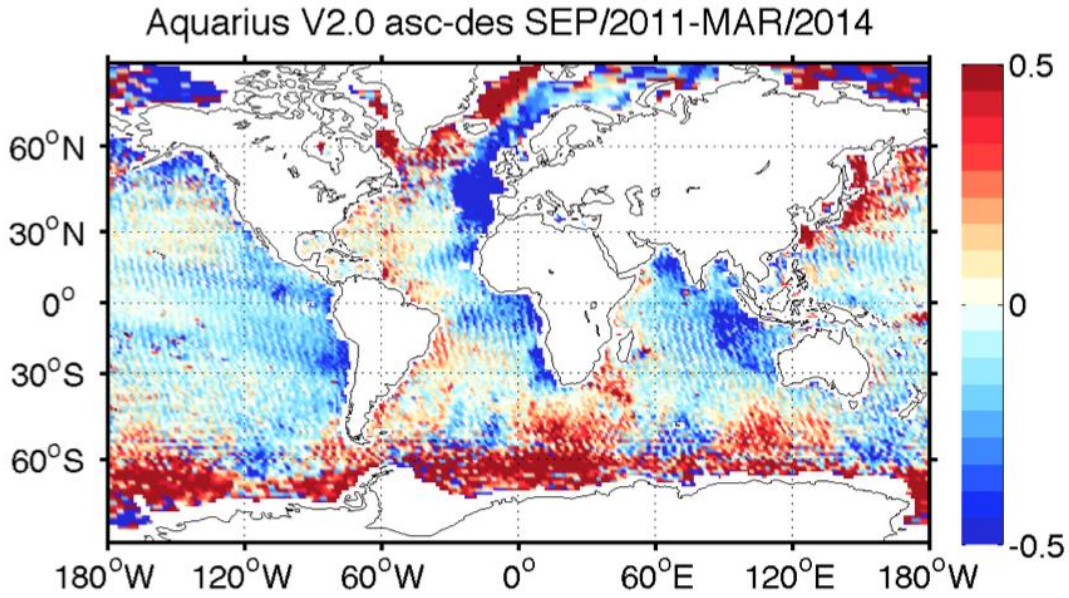

Figure 9. 31-month average Ascending – Descending V2.0 data. Major bias regions are described in the text.

Figure 10 shows that in V4.0 the RFI influenced areas, including the both sides of the Atlantic Ocean, eastern Indian Ocean, and the northwestern Pacific are masked out for the large ascending minus descending biases. The biases in the extreme Northern Hemisphere are essentially unchanged. The positive biases (>0.5 psu) in the southern ocean for V2.0 have been significantly reduced in V4.0 (<0.2 psu) after improving the galaxy correction.

There are small but visible asc-dsc biases at high southern latitudes that remain in V4.0. One can see a zonal variation between light blue and light red blobs around 60°S. It is not clear at this point what the reasons are for these asc-dsc biases.

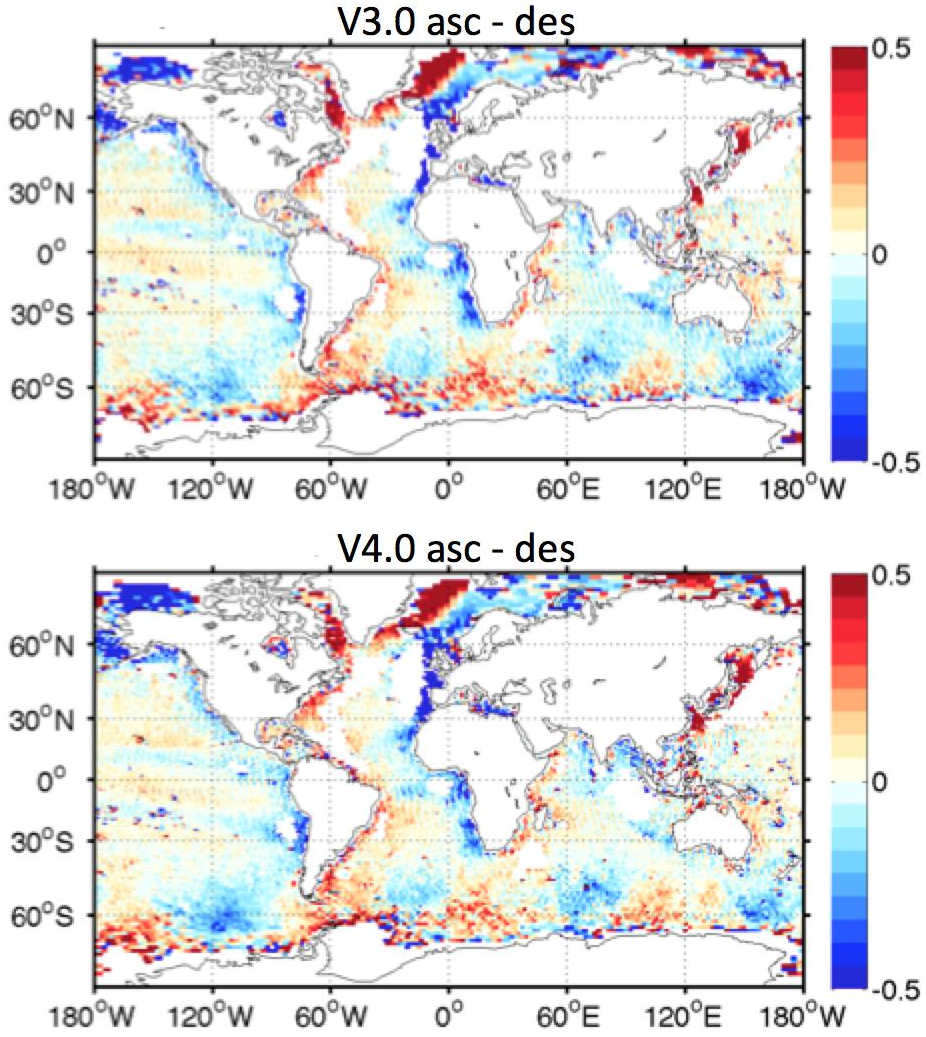

Figure 10. Same as Figure 9 for Aquarius V3.0 and V4.0 data averaged from SEP/2011-Jan/2015. The "white" regions in the North Atlantic, Western Pacific (China, Japan) or Indonesia are masked out due to suspected undetected RFI. See flagging/masking tables in [9] for details.

Figures 11-13 show the buoy difference statistics in discrete latitude bands for ascending, descending and both (entire orbit), and for the V2.0, V3.0 and V4.0 data, respectively. V2.0 ascending biases are negative (~-0.2 psu) in the tropics and positive (~0.2 psu) at 40°S and 40°N. Standard deviations are lower in the tropics and higher in the high latitudes. The V3.0/V4.0 standard deviations are reduced around 0.05 in the tropics to 0.25 in high latitudes relative to V2.0. The latitudinal biases are almost identical in the ascending and descending passes in V3.0/V4.0. The standard deviations are about the same in V3.0 and V4.0. The latitudinal biases that are obvious in V3.0 (Figure 12) are significantly reduced in V4.0 with the updated geophysical model function (GMF) to correct SST and wind effect on roughness in V4.0.

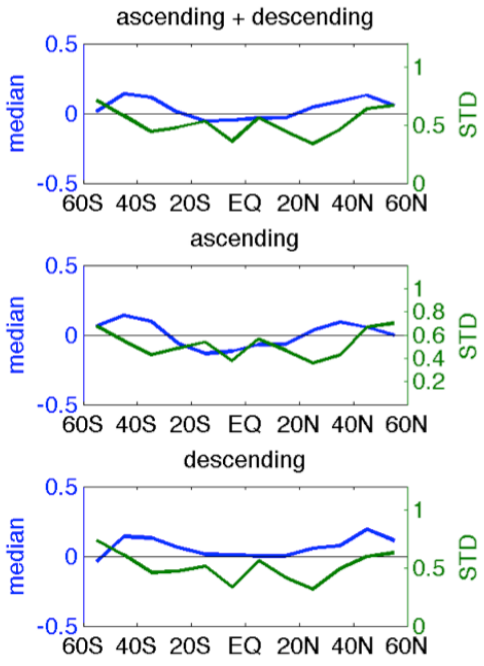

STD	both	ascend	descen
50-60N	0.67	0.70	0.63
40-50N	0.64	0.67	0.60
30-40N	0.46	0.43	0.49
20-30N	0.34	0.36	0.32
10-20N	0.44	0.47	0.41
0-10N	0.56	0.57	0.56
10S-0	0.36	0.38	0.33
10-20S	0.53	0.54	0.52
20-30S	0.48	0.48	0.47
30-40S	0.45	0.43	0.46
40-50S	0.58	0.55	0.61
50-60S	0.71	0.68	0.73

Figure 11. Aquarius V2.0 gridded data co-located buoy differences by latitude bands, all data from Sep 2011 through Mar 2014.

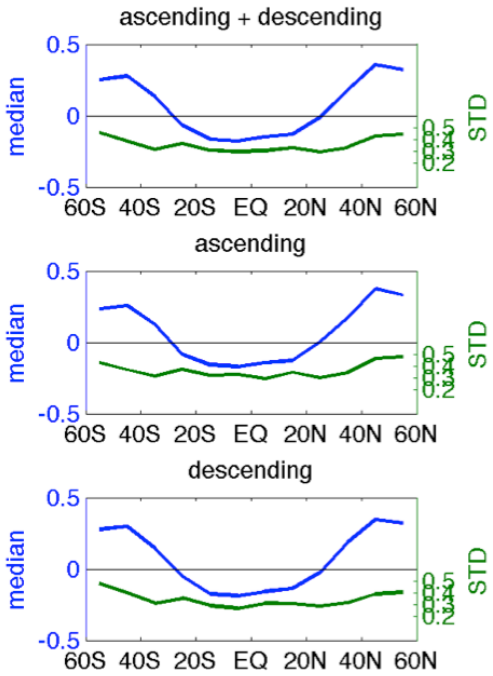

STD	both	ascend	descen
50-60N	0.44	0.48	0.40
40-50N	0.43	0.46	0.39
30-40N	0.33	0.35	0.32
20-30N	0.29	0.30	0.29
10-20N	0.33	0.35	0.31
0-10N	0.30	0.30	0.31
10S-0	0.30	0.33	0.27
10-20S	0.31	0.32	0.29
20-30S	0.36	0.37	0.36
30-40S	0.31	0.31	0.31
40-50S	0.39	0.37	0.40
50-60S	0.45	0.43	0.48

Figure 12. Same as Figure 11 for Aquarius V3.0 data.

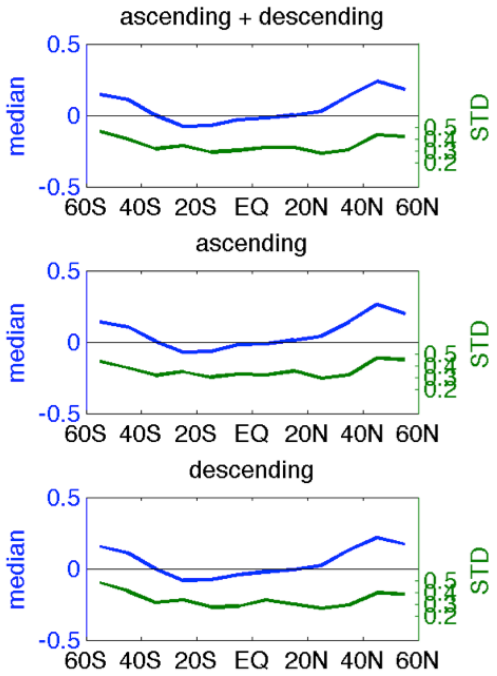

STD	both	ascend	descen
50-60N	0.42	0.45	0.39
40-50N	0.44	0.47	0.40
30-40N	0.31	0.32	0.29
20-30N	0.28	0.29	0.26
10-20N	0.33	0.35	0.30
0-10N	0.33	0.32	0.33
10S-0	0.30	0.33	0.28
10-20S	0.29	0.31	0.28
20-30S	0.34	0.35	0.34
30-40S	0.32	0.32	0.32
40-50S	0.40	0.38	0.41
50-60S	0.46	0.44	0.48

Figure 13. Same as Figure 11 for Aquarius V4.0 data.

8. Ascending – descending bias variations over time

Figure 14-16 contrast the variability of V2.0 and V4.0 global average deviations from buoy measurements in ascending-only matchups, descending-only, and the ascending-descending differences. Figure 14 shows the annual variations in both ascending and descending orbits in V2.0. In ascending passes, negative biases show up in every August. In descending passes, positive biases show up in every April. One sees that the improved galaxy correction in V4.0 provides time series with no seasonal variations in Figure 14, 15. Figure 16 shows that the annual variability of ascending minus descending differences for up to 0.4 psu in V2.0 are gone in V3.0 and V4.0, showing that the quasi-seasonal variations due to galaxy were mostly corrected in V3.0.

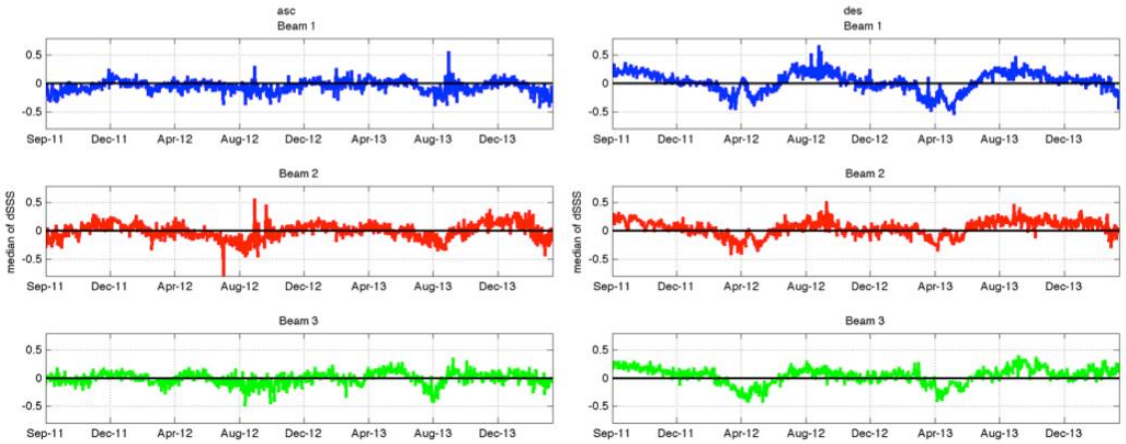

Figure 14. Daily average ascending (left) and descending (right) Aquarius – buoy difference time series, V2.0 data.

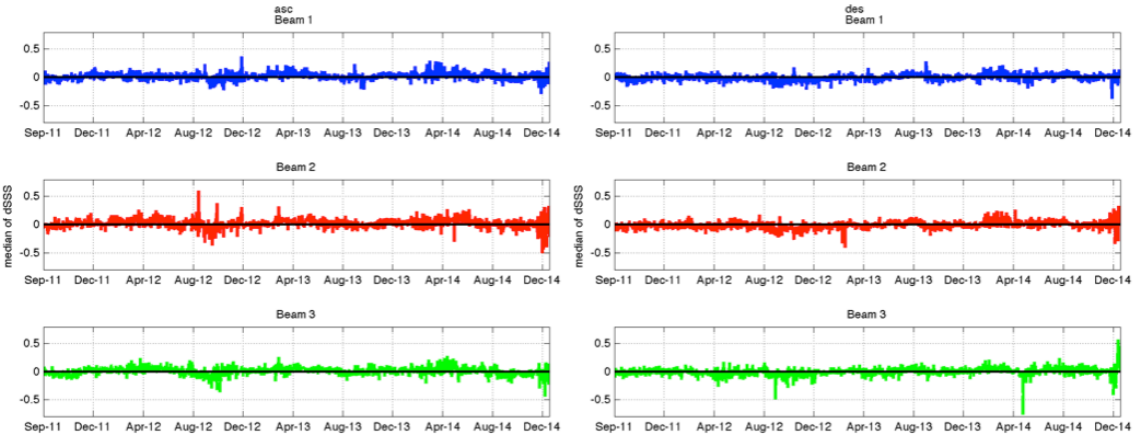

Figure 15. Same as Figure 14 for Aquarius V4.0 data.

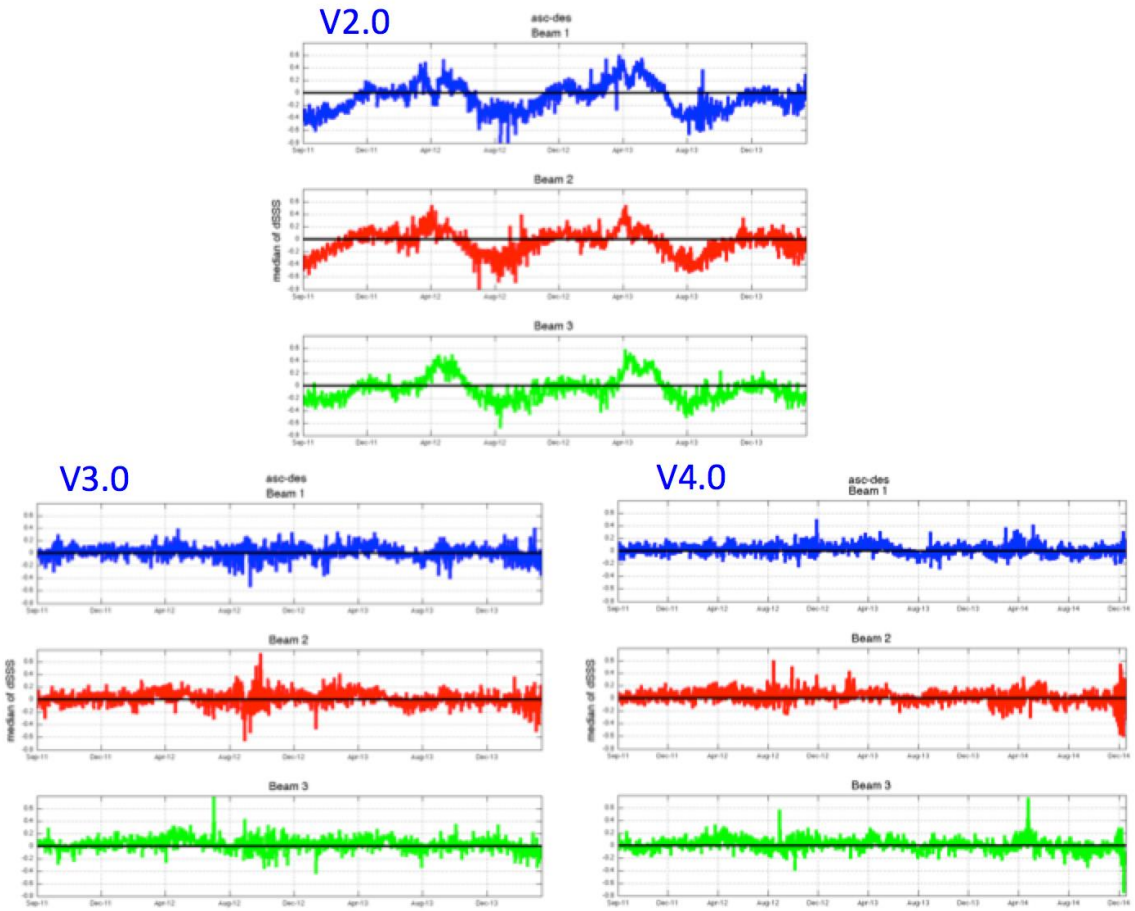

Figure 16. Daily average ascending minus descending Aquarius-buoy difference time series for Aquarius V2.0 (upper), V3.0 (bottom left) and V4.0 (bottom right).

Figure 17 shows V2.0 and V4.0 ascending–descending maps for the month of October 2011. The remaining biases in V4.0 show up near the coasts due to the unknown RFI. The ascending and descending differences are much smaller in V4.0 than in V2.0. The biases are less than 0.2 psu in the open oceans.

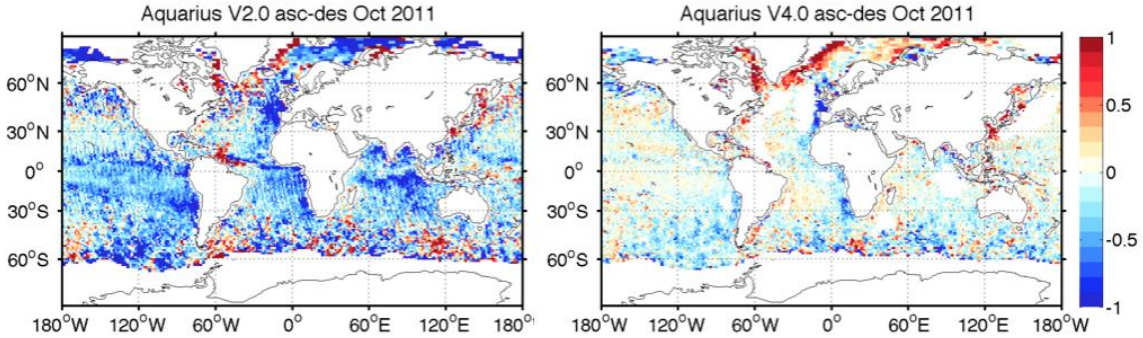

Figure 17. Ascending minus descending maps for October 2011 showing significant improvement in V4.0 compared to V2.0. The "white" regions in the North Atlantic, Western Pacific (China, Japan) or Indonesia are masked out due to suspected undetected RFI. See flagging/masking tables in [9] for details.

In Figure 18 is utilized to illustrate the magnitude and geographic pattern of the seasonal ascending –descending changes on a monthly basis. The seasonal variations of the biases in the Southern Hemisphere are still observed, but the amplitude has been reduced from larger than 1 psu in V2.0 to less than 0.5 psu in V4.0. The Northern Hemisphere RFI zones described earlier are still persistent year-round.

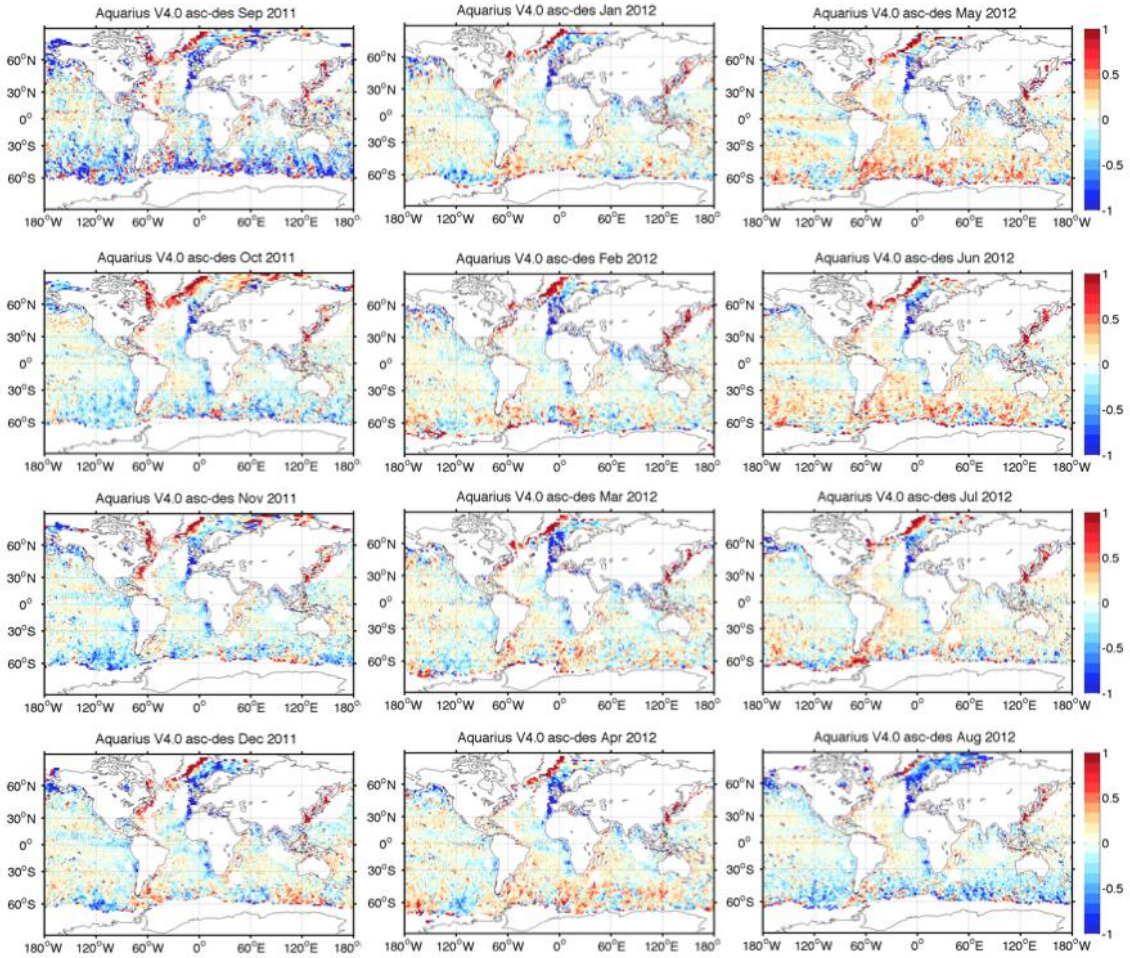

Figure 18. V4.0 ascending minus descending maps for September 2011 through August 2012 showing the seasonal progression.

9. Quantitative error assessments for gridded data

This next discussion compiles results of buoy collocation differences by month, season and latitude bands to quantitatively assess the V4.0 errors relative to the mission accuracy requirements. ESR gridded maps are used and three monthly maps are averaged for seasonal analyses. As noted above, the buoy matchups are compiled for each 1-degree grid with an average of the buoys within the 150 km radius and with buoy SST>5°C. In some tabulations we also compute the expected value of the buoy standard deviations for the grid point matchups.

Figure 19 shows the seasonal-average buoy difference compilations, again demonstrating the annual variation of the salinity errors. Figure 20 provides latitude distributions for the four seasons of Aquarius-buoy bias and standard deviations. The biases are significantly reduced compared to V2.0. The range of the color bar is changed to -0.5 to 0.5 to show the remaining biases in the high latitude. The standard deviations are lower than 0.2 psu for most of the areas. Table 3 lists all the numerical values for season and latitude band, and highlights those where both the bias and standard deviation are at or less than 0.2, comprising 75% of the cases (comparing to 25% in V2.0).

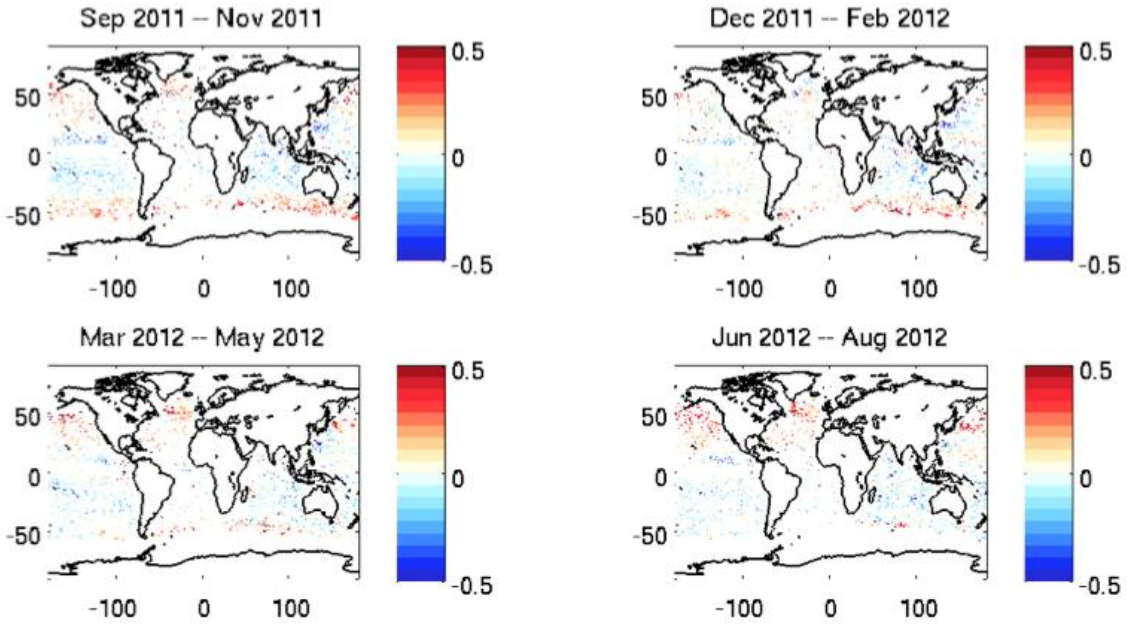

Figure 19. V4.0 Aquarius seasonal buoy difference maps in the first year.

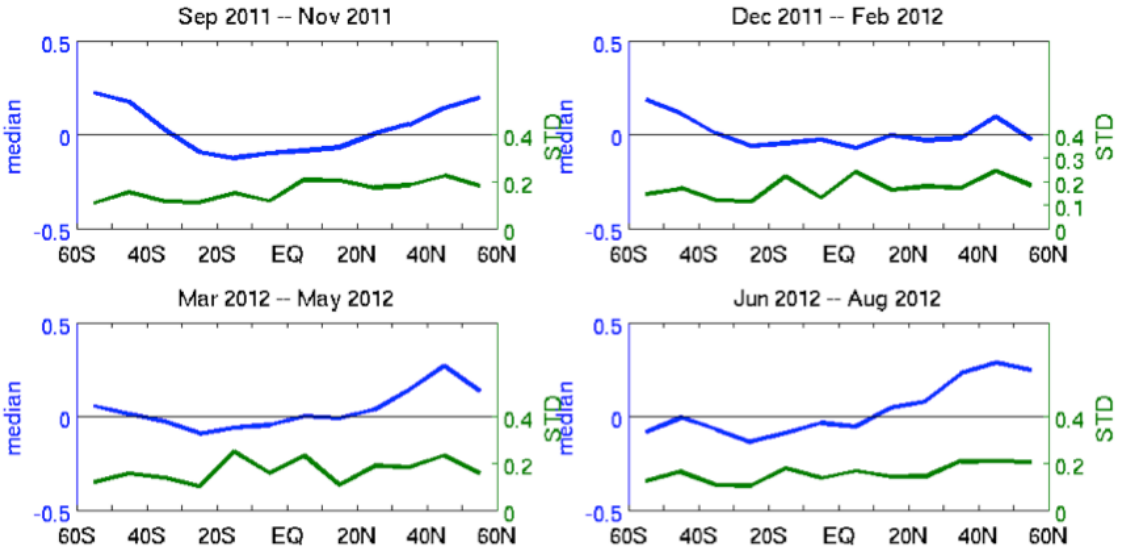

Figure 20. Seasonal average buoy differences by latitude range.

Table 4. Co-located buoy differences for Aquarius V4.0 seasonal average gridded maps, by latitude zones. Highlighted values have bias and standard deviation both within 0.2 psu.

Latitude	SON Bias/STD		DJF Bias/STD		MAM Bias/STD		JJA Bias/STD	
50-60N	0.19	0.18	-0.03	0.18	0.14	0.16	0.25	0.20
40-50N	0.14	0.22	0.10	0.25	0.27	0.23	0.29	0.21
30-40N	0.05	0.19	-0.02	0.17	0.14	0.18	0.23	0.21
20-30N	0.00	0.17	-0.03	0.18	0.04	0.19	0.08	0.14
10-20N	-0.07	0.20	0.00	0.16	-0.1	0.11	0.05	0.14
0-10N	-0.08	0.21	-0.07	0.24	0.00	0.23	-0.05	0.17
10S-0	-0.10	0.12	-0.03	0.13	-0.05	0.16	-0.04	0.14
10-20S	-0.12	0.15	-0.05	0.22	-0.06	0.25	-0.09	0.18
20-30S	-0.09	0.11	-0.06	0.12	-0.10	0.10	-0.14	0.10
30-40S	0.03	0.12	0.01	0.12	-0.03	0.14	-0.07	0.11
40-50S	0.17	0.15	0.11	0.17	0.01	0.16	-0.1	0.16
50-60S	0.22	0.11	0.18	0.15	0.05	0.12	-0.08	0.12

In table 5, the latitude bands are consolidated between hemisphere, and we also give the estimated buoy standard deviations within those latitude bands. The buoy standard deviations at each grid point are calculated from the entire buoy SSS value within the 150 km searching radius. From these we estimate the Aquarius standard deviations as the square-root of the difference between the Aquarius–buoy variance and the buoy variance.

$$\text{Aquarius\_error} = \text{sqrt}(\text{Aquarius-buoy\_STD}^2 - \text{buoy\_STD}^2) \qquad (1)$$

These are shown in Table 6, which shows them in reference to the error budget analysis for the mission accuracy requirements. This shows an error allocation by latitude that provides the 0.2 psu global RMS error. Our seasonal mean global RMS estimates are currently about 0.14.

An alternate analysis is provided in Table 7 and 8. Here we use the triple point analysis, as above in Section 4, to estimate the global RMS error for 24 months and 12 seasons. The average Aquarius RMSE for the seasonal and monthly Level 3 gridded data are ~0.16 and ~0.17 (range between 0.13 and 0.20) psu respectively,

which are considerably less than the Level 2 point measurements ~0.28 psu presented in Table 1.

Table 5. Seasonal average buoy difference statistics for V4.0 gridded data in consolidated latitude bands (Bias and STD), and buoy standard deviations (STDb).

Latitude	SON			DJF			MAM			JJA		
	BIAS	STD	STDb	BIAS	STD	STDb	BIAS	STD	STDb	BIAS	STD	STDb
0-10	-0.10	0.17	0.17	-0.04	0.19	0.17	-0.03	0.20	0.18	-0.04	0.15	0.15
11-20	-0.11	0.18	0.11	-0.03	0.20	0.13	-0.04	0.20	0.12	-0.04	0.17	0.12
21-30	-0.07	0.15	0.09	-0.05	0.15	0.09	-0.03	0.16	0.09	-0.06	0.16	0.10
31-40	0.03	0.14	0.08	0.00	0.14	0.09	0.03	0.18	0.08	0.03	0.22	0.10
41-50	0.17	0.18	0.09	0.11	0.19	0.09	0.07	0.22	0.10	0.06	0.22	0.11
51-60	0.22	0.15	0.08	0.16	0.18	0.06	0.08	0.14	0.06	0.07	0.23	0.10

Table 6. Seasonal standard deviations (STDa) error estimates compared with Minimum Mission Requirements.

Minimum Mission Seasonal Salinity Error (psu)		SON	DJF	MAM	JJA
Latitude range	Allocation (psu)	STDa	STDa	STDa	STDa
0-10	0.15	0	0.08	0.09	0
11-20	0.16	0.14	0.15	0.16	0.12
21-30	0.16	0.12	0.12	0.13	0.12
31-40	0.18	0.11	0.11	0.16	0.20
41-50	0.21	0.16	0.17	0.20	0.19
51-60	0.24	0.13	0.17	0.13	0.21
61-70	0.26				
Global RMS	0.20	0.12	0.14	0.15	0.16

Table 7. Triple point analysis for monthly global RMS errors for Aquarius V4.0 data for 24 months.

Yr-Month	Aquarius	HYCOM	BUOY	Yr-Month	Aquarius	HYCOM	BUOY
	RMSE	RMSE	RMSE		RMSE	RMSE	RMSE
11-Sep	0.16	0.17	0.11	12-Sep	0.16	0.16	0.15
11-Oct	0.17	0.17	0.12	12-Oct	0.18	0.16	0.14
11-Nov	0.19	0.15	0.13	12-Nov	0.16	0.17	0.17
11-Dec	0.16	0.13	0.15	12-Dec	0.16	0.16	0.14
12-Jan	0.14	0.15	0.13	13-Jan	0.14	0.17	0.11
12-Feb	0.13	0.15	0.13	13-Feb	0.11	0.14	0.11
12-Mar	0.14	0.14	0.13	13-Mar	0.15	0.11	0.11
12-Apr	0.17	0.14	0.12	13-Apr	0.17	0.11	0.09
12-May	0.18	0.13	0.13	13-May	0.16	0.11	0.11
12-Jun	0.20	0.12	0.14	13-Jun	0.19	0.11	0.11
12-Jul	0.17	0.16	0.12	13-Jul	0.17	0.08	0.17
12-Aug	0.14	0.16	0.14	13-Aug	0.14	0.11	0.13

Table 8. Triple point analysis for seasonal global RMS errors for Aquarius V4.0 data.

2011-14 Season	Aquarius	HYCOM	BUOY
	RMSE	RMSE	RMSE
SON	0.16	0.15	0.15
D(1)JF(2)	0.14	0.13	0.13
MAM	0.16	0.12	0.12
JJA	0.16	0.14	0.14
SON	0.16	0.16	0.16
D(2)JF(3)	0.13	0.13	0.12
MAM	0.15	0.10	0.10
JJA	0.15	0.09	0.14
SON	0.15	0.11	0.14
D(3)JF(4)	0.14	0.08	0.16
MAM	0.17	0.09	0.19
JJA	0.16	0.08	0.22

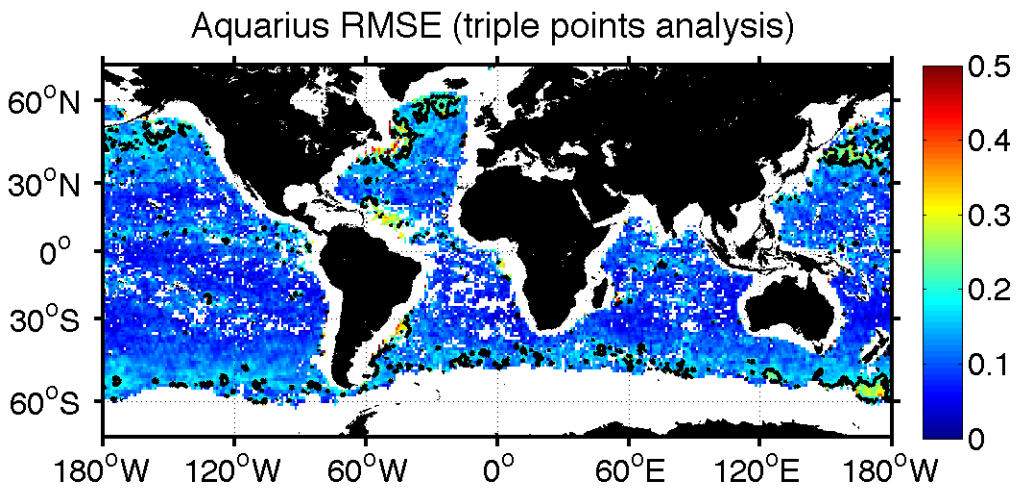

Figure 21. Global map of Aquarius RMSE calculated from triple point analysis from Sep/2011-Aug/2014.

Figure 21 shows at each grid point the estimated RMSE in the Aquarius SSS based on the triple collocation method. It demonstrates the locations on the Earth where we meet the 0.2 psu (blue color) requirements and where the data still need improvement. The black contours indicate the 0.2 psu. In the open ocean, the RMSE are generally lower than 0.2 psu. Some high RMSE areas include the Amazon plume (may be due to stratification and temporal variability), northwestern Atlantic (strong RFI), and the North Pacific (SST-related).

10. Mission science requirements & compliance matrix

The Aquarius mission science requirements matrix is shown in Table 9. The two right-hand columns indicate the Baseline and Minimum mission. The fundamental science requirement is to achieve global RMS random errors and systematic biases no larger than 0.2 psu on 150 km by 150 km scales over the open ocean. The baseline mission requires this on a monthly average, and the minimum mission requires on a seasonal (3-month) average. The triple point analyses presented in Section 9 above indicate that V4.0 global RMS error is ~0.17 monthly and ~0.16 seasonally.

Table 9. Aquarius Mission Science Requirements compliance matrix. The Minimum Mission duration and data product delivery requirements are met. The rms error requirement of 0.2 psu is fully achieved with V4.0.

	Level 1 Science Mission Requirement	Baseline Mission	Minimum Mission
1	The Aquarius Mission shall collect the space-based measurements to retrieve Sea Surface Salinity (SSS) with global root-mean-square (rms) random errors and systematic biases no larger than 0.2 psu on 150 km by 150 km scales over the open ocean.	V2.0: 0.30	V2.0: 0.27
		V3.0 0.24	V3.0 0.23
		V4.0: 0.17	V4.0: 0.16
2	SSS Averaging Interval	1 Month	3 Months
3	Mission Duration	At least 3 Years	At least 1 Year

11. Validation for sea surface density

Using Aquarius salinity data and the ancillary SST (Reynolds SST), we are able to calculate the value of sea surface density. Here we use Thermodynamic Equation Of Seawater - 2010 (TEOS-10) which is based on a Gibbs function formulation [10]. The density unit is kg m^{-3}.

Figure 22 shows the density at the buoy matchup points for the 41 months of observations. The *in situ* density is computed from *in situ* SSS and ancillary SST to exclude the variance in the density due to the differences between *in situ* SST and ancillary SST. The two density maps look quite similar, except the density maps from Aquarius show higher density in high latitude and lower density in the tropics. The density bias corresponds to the salinity biases in Aquarius.

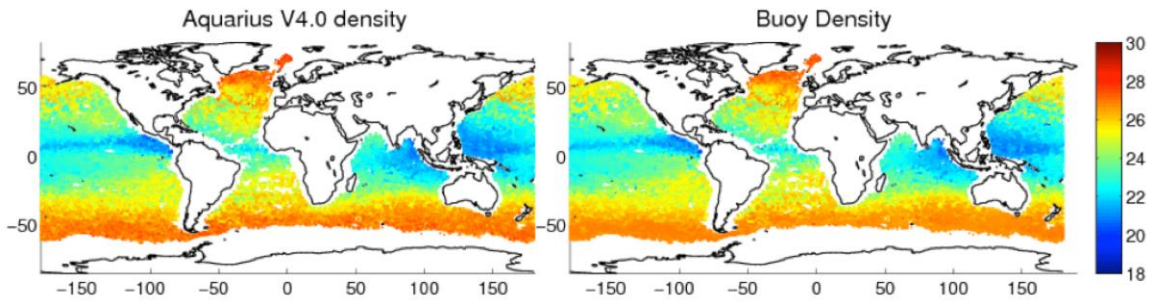

Figure 22. Aquarius and buoy co-located density data. The unit is density-1000 (kg m^{-3}).

Figure 23 shows the global map of density differences, which shows the similar patterns to the global map of salinity differences (Figure 2).

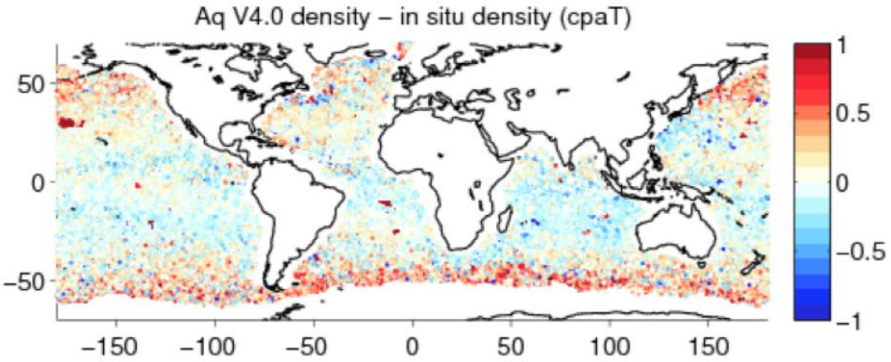

Figure 23. Global map of density differences.

Figure 24 shows the time series of global daily median values of density differences. The density biases are close to zero similar to the salinity biases in Figure 7.

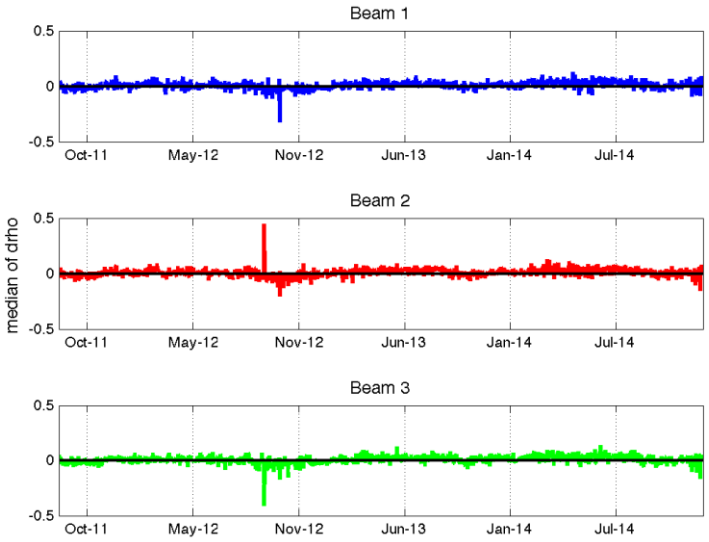

Figure 24. Daily bias of density (Aquarius – in situ).

Histograms of the matchup salinity differences for each of the three beams are in Figure 25. The standard deviations are ~0.27.

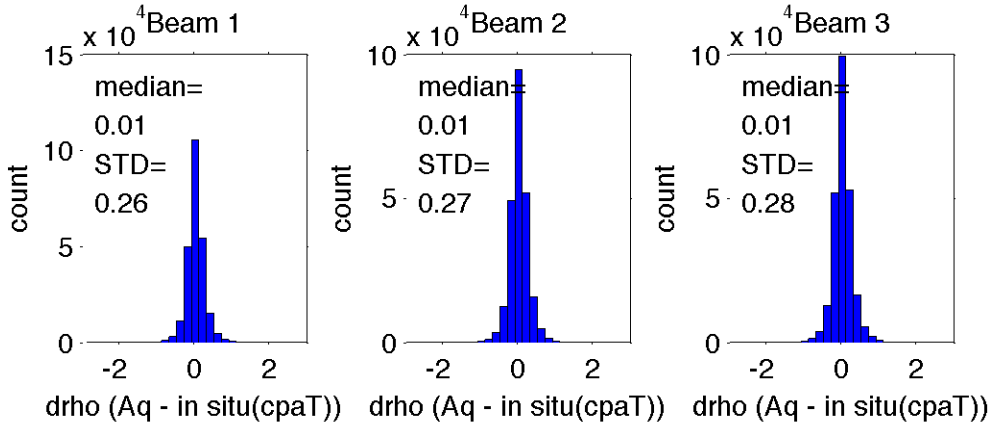

Figure 25. Histograms for Aquarius – buoy differences. In situ density calculated from insitu S and *reference T.*

Figure 24 shows the seasonal density differences maps (contributed by Jorge Vazquez). Note that the maps show the differences of Argo minus Aquarius density, so the sign is the opposite compared to the salinity differences shown in Figure 8. Similar patterns are observed for salinity and density differences. For example, the Aquarius has higher values in the Southern Ocean in fall and in winter, and in the north Pacific during the boreal summer.

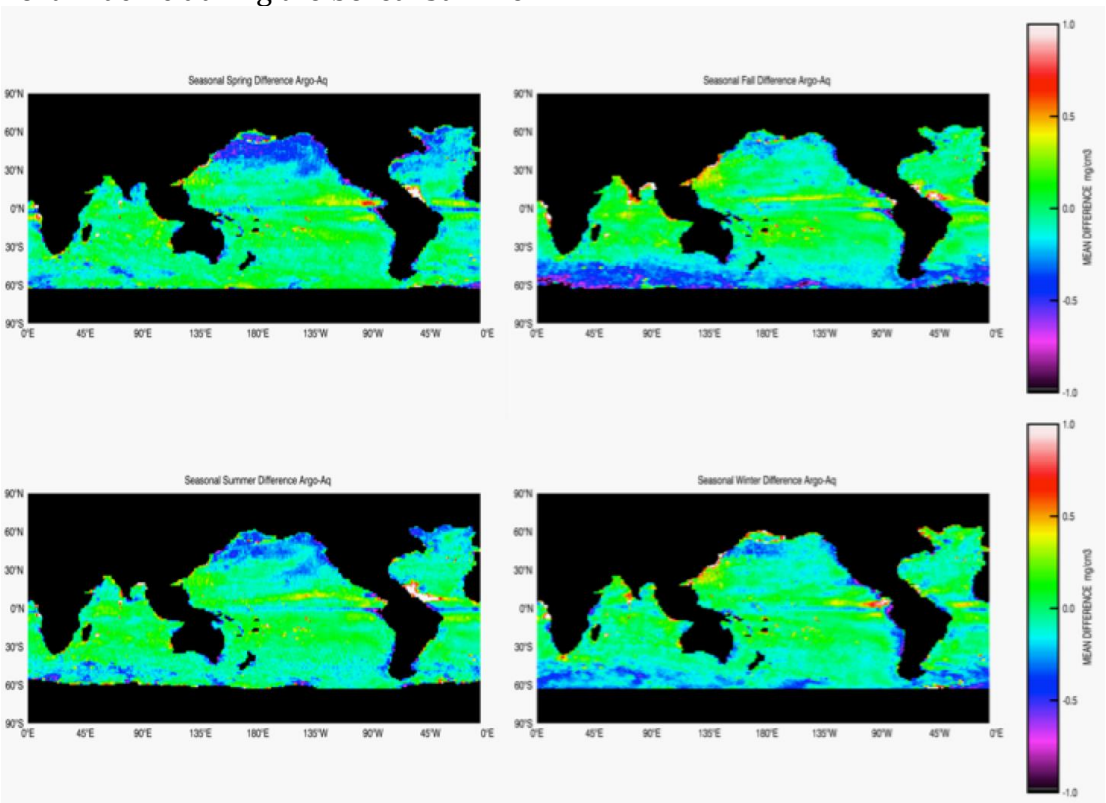

Figure 26. Maps of seasonal density biases. Data processing by Jorge Vazquez.

Figure 27 shows the maps of seasonal density RMS of the differences. The large RMS regions include the North Pacific in spring, Southern Ocean in fall and eastern equatorial Pacific in winter-spring. The RMS is generally under 0.2 in the open ocean.

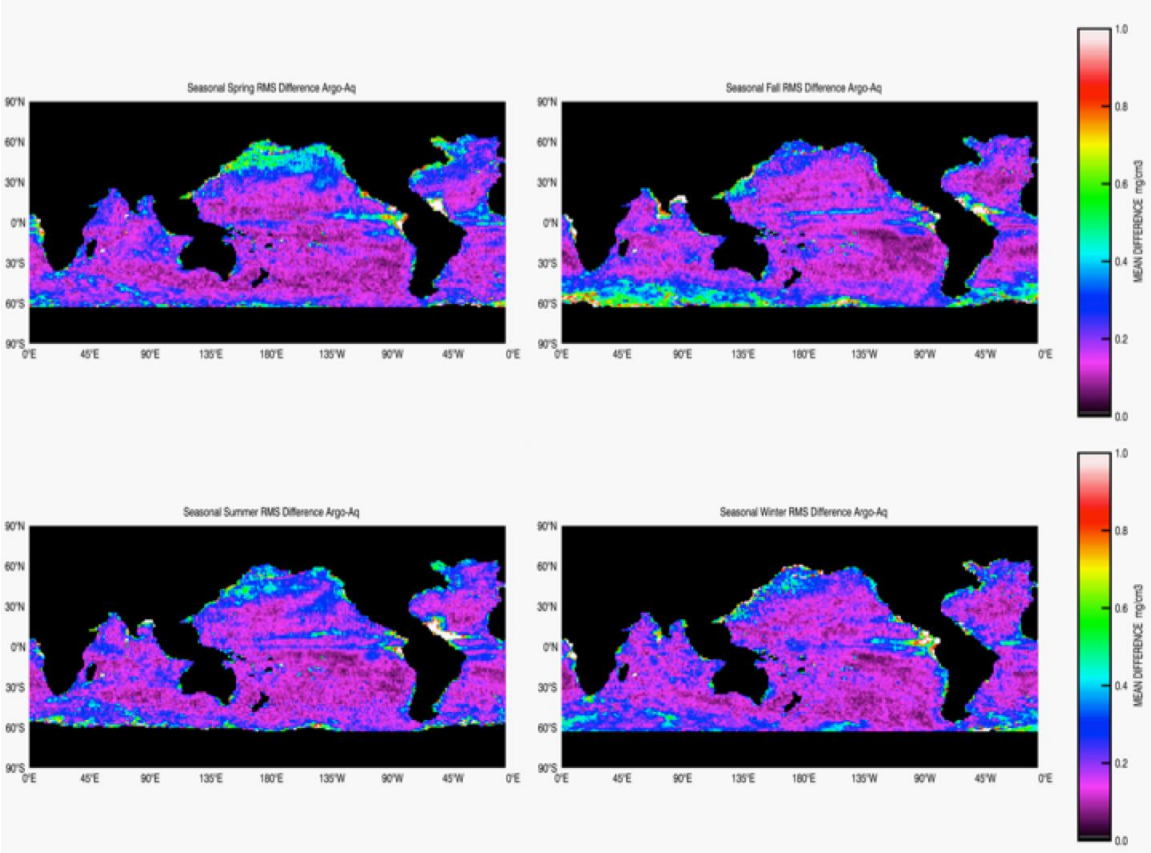

Figure 27. Maps of seasonal density RMS of the differences. Data processing by Jorge Vazquez.

12. Summary, conclusions and cautions

This analysis documents the improvements in the V4.0 science data processing and their effect on Aquarius salinity data. By various measures, the RMS errors are reduced significantly relative to V2.0. With V4.0, we find that the global RMS error is ~0.17 psu monthly and ~0.16 psu seasonally for data that are gridded and smoothed with a 150 km scale.

Localized persistent biases between ascending and descending passes appear to be linked to radio frequency interference (RFI) that is not completely corrected by the RFI filter. The RFI will bias the brightness temperatures toward the positive, thus the salinity will be biased negative. These regions are primarily in the eastern N. Atlantic adjacent to Europe where it is likely that the ascending pass is contaminated as the antenna faces the European subcontinent. Likewise, the western N. Atlantic and Asia-Pacific regions are biased on the descending pass when the antenna views westward. In V4.0, Flag #23 is added to exclude the area with

unacceptable asc/dsc differences. This flag identifies areas where the asc/dsc difference is sufficiently large that the data from the out-of-bound pass (i.e. either asc or dsc) is discarded for purposes of calibration. The algorithm is to be provided by T. Meissner. Figure 5 shows that the eastern N. Atlantic and the eastern N. Indian Ocean are masked out in the ascending map, and the western N. Atlantic and Pacific are masked out in the descending map.

Note of Caution, RFI: Persistent negative salinity bias may be present in some regions due to RFI. Users should be very cautious with using ascending pass data in the eastern N. Atlantic and descending pass data in the western N. Atlantic and Asia-Pacific regions.

Note of Caution, latitudinal biases: V3.0 shows salty biases at high N latitude (in particular the N Pacific). The biases are related to SST, possibly due to surface roughness or air-sea temperature difference or a combination of both. V4.0 take care of many biases that simply correlated with SST (dielectric model, O_2) though issues with the roughness correction (e.g. air-sea temperature) might still remain.

13. Reference

1. Lagerloef, G., R. Colomb, D. Le Vine , F. Wentz , S. Yueh, C. Ruf, J. Lilly, J. Gunn , Y. Chao, A. de Charon , G. Feldman, and C. Swift; The Aquarius/SAC-D mission –Designed to Meet the Salinity Remote Sensing Challenge, Oceanography, Volume 21(1), 68-81, 2008.
2. Le Vine, D.M., G.S.E. Lagerloef, F.R. Colomb, S.H. Yueh, and F.A. Pellerano. 2007. Aquarius: An instrument to monitor sea surface salinity from Space IEEE Transactions on Geoscience and Remote Sensing 45 (7):2,040–2,050.
3. Aquarius V4.0 Algorithm Theoretical Basis Document (ATBD)
4. Aquarius Radiometer Post-Launch Calibration for Product Version 2 [AQ-014-PS-0015]
5. Reynolds, R. W., T. M. Smith, C. Liu, D. B. Chelton, K. S. Casey, and M. G. Schlax, 2007: Daily high-resolution blended analyses for sea surface temperature. J. Climate, 20, 5473-5496.
6. Chassignet, E.P., H.E. Hurlburt, E.J. Metzger, O.M. Smedstad, J. Cummings, G.R. Halliwell, R. Bleck, R. Baraille, A.J. Wallcraft, C. Lozano, H.L. Tolman, A. Srinivasan, S. Hankin, P. Cornillon, R. Weisberg, A. Barth, R. He, F. Werner, and J. Wilkin, 2009. U.S. GODAE: Global Ocean Prediction with the HYbrid Coordinate Ocean Model (HYCOM). Oceanography, 22(2), 64-75.
7. E.J. Metzger, O.M. Smedstad, P. Thoppil, H.E. Hurlburt, A.J. Wallcraft, D.S. Franklin, J.F. Shriver, and L.F. Smedstad, 2008: Validation Test Report for the Global Ocean Prediction System V3.0 – 1/12° HYCOM/NCODA: Phase I. NRL Memo. Report, NRL/MR/7320--08-9148.
8. E.J. Metzger, O.M. Smedstad, P.G. Thoppil, H.E. Hurlburt, D.S. Franklin, G. Peggion, J.F. Shriver, T.L. Townsend, and A.J. Wallcraft, 2008: Validation

Test Report for the Global Ocean Prediction System V3.0 – 1/12° HYCOM/NCODA: Phase II. NRL/MR/7320--10-9236.
9. Aquarius Level-2 Data Product, Version 4.0 [AQ-014-PS-0018]
10. IOC, SCOR and IAPSO, 2010: The international thermodynamic equation of seawater – 2010: Calculation and use of thermodynamic properties. Intergovernmental Oceanographic Commission, Manuals and Guides No. 56, UNESCO (English), 196 pp. [www.teos-10.org/pubs/TEOS-10_Manual.pdf]

Appendix A: The NAVO/FSU HYCOM data are obtained from the global 1/12° data-assimilative HYCOM model along with the Navy Coupled Ocean Data Assimilation (NCODA) system at the Naval Oceanographic Office (NAVOCEANO). The HYCOM data are available from the HYCOM data server http://tds.hycom.org/thredds/GLBa0.08/expt_90.9.html?dataset=GLBa0.08/expt_90.9

This HYCOM run assimilates available along track satellite altimeter observations, satellite and *in situ* sea surface temperature as well as in situ vertical temperature and salinity profiles from XBTs, ARGO floats, and moored buoys. In terms of near surface salinity forcing, HYCOM uses monthly climatology of river discharges (applied at the top 6 meters of the model) and relaxation to monthly SSS climatology (at 15 m) with a restoring time scale of 30 days, in addition to E-P forcing. Both the climatological river forcing and near surface salinity relaxation are intended to prevent the HYCOM simulation from drifting away from climatology, but at the same time they may suppress non-seasonal variations occurring in nature. The NCODA system is based on a multi-variate Optimal Interpolation (MVOI) scheme. Because of the assimilation of Argo floats and buoy data, the HYCOM analysis is not independent of Argo and buoys. Moreover, the nature of the assimilation could also introduce some level of correlation between the errors of the HYCOM analysis field and the errors of Argo and buoy SSS. More details of this HYCOM solution can be found in [6], [9] and [10].

Appendix B: Triple point uncertainty estimate of Aquarius and validation data

The satellite salinity measurement S_S and the *in situ* validation measurement S_V are defined by:

$$S_S = S \pm \varepsilon_S$$
$$S_V = S \pm \varepsilon_V$$

where S is the true surface salinity averaged over the Aquarius footprint area and microwave optical depth in sea water (~1cm). ε_S and ε_V are the respective satellite and in situ measurement errors relative to S. The mean square of the difference ΔS between S_S and S_V is given by:

$$\langle \Delta S_{SV}^2 \rangle = \langle \varepsilon_S^2 \rangle + \langle \varepsilon_V^2 \rangle \qquad (1)$$

where < > denotes the average over a given set of paired satellite and *in situ* measurements, and $<\varepsilon_S \varepsilon_V> = 0$. Likewise, define HYCOM salinity interpolated to the satellite footprint as $S_H = S \pm \varepsilon_H$, and mean square differences

$<\Delta S_{HV}^2> = <\varepsilon_H^2> + <\varepsilon_V^2>$ (2) HYCOM vs *in situ* validation data

$<\Delta S_{SH}^2> = <\varepsilon_S^2> + <\varepsilon_H^2>$ (3) satellite vs HYCOM

Equations (1) – (3) comprise three equations with three variables given by:

$< \varepsilon_S^2> = \{ <\Delta S_{SV}^2> + < \Delta S_{SH}^2> - <\Delta S_{HV}^2>\} /2$ (4) satellite measurement error

$< \varepsilon_H^2> = \{ <\Delta S_{SH}^2> + < \Delta S_{HV}^2> - <\Delta S_{SV}^2>\} /2$ (5) HYCOM measurement error

$< \varepsilon_V^2> = \{ <\Delta S_{SV}^2> + < \Delta S_{HV}^2> - <\Delta S_{SH}^2>\} /2$ (6) *in situ* validation measurement error

End of document